TRANSPARENT INSULATION MATERIALS IN BUILDING RETROFIT: POTENTIALS FOR TERRASSENHAUSSIEDLUNG GRAZ

A. Eberl[1]
[1]Institute of Buildings and Energy, TU Graz, Graz, Austria
E-Mail: alexander.eberl@tugraz.at

ABSTRACT

This paper investigates the potential of 3 market available transparent insulation materials (TIM) in building retrofit by the case study of the iconic 1970ies housing estate Terrassenhaussiedlung in Graz, Austria. To achieve this, different façade configurations are modeled in a 2D-simulation environment (HTflux) and tested in a dynamic simulation environment (IESVE) for different orientations and overshading situations. The results show that that even low-tech TIM can outperform conventional insulation materials in terms of heating energy demand, when applied to façade areas with high solar exposure, while only transparent aerogel can compete with conventional insulation materials on badly exposed areas.

INTRODUCTION

This paper investigates passive solar retrofit scenarios for the 1970ies housing estate *Terrassenhaussiedlung*, a highly recognized example of late modernist architecture in Graz, Austria. Following the idea of a "megastructure" it consists of a clearly visible primary structure, materialised in exposed concrete, which is contrasted by a secondary structure of lightweight "infills" (see Figure 1).

The hypothesis is of this work is, that TIM could be part of a strategy to modernize the estate in an energy-efficient and at the same time heritage sensitive way: Instead of insulating the entire building envelope, only parts of the façade are modified towards passive solar gains. It is assumed that higher thermal losses, when compared to common insulation measures, can be partially or even fully compensated by solar gains. To verify this hypothesis, different variations of solar façade systems are modelled, tested in a static (HTflux) and a dynamic simulation environment (IESVE) and compared to common insulation measures.

Literature Review

The advantages of TIM and TI-facades have been thoroughly described in the literature. Most literature about this topic was published between the mid-1990ies and mid-2000s in Germany with Fraunhofer ISE in Freiburg and University of Karlsruhe being very active in that field (Wagner 1998, Kerschberger et al. 1998., Reiß et al 2005). At present Brno University of Technology in Czech Republic is very active in the research of TIM and solar façades (Čekon et al. 2020, Čekon and Čurpek 2019).

Figure 1: Terrassenhaussiedlung Graz

Currently there are 4 types of transparent insulation materials on the market:

1. capillary mats and honeycomb structures
2. polycarbonate sheets
3. Fleeces and fibers
4. Silica Aerogel granulate

All these systems have already been described in the literature more than 20 years ago. In fact, only a small portion of the products and systems described in the early literature (Kerschberger 1998, Wagner 1998, Maiwald 2000, Reiss et al. 2005) are still available. Large competitors like *Sto* and *BASF* have retreated from the market and only a few products survived in the niche of translucent daylighting systems.

Reasons for the bad success of these systems are manifold. As stated by Platzer (1998) there are issues with building regulations, high investment costs, and systems are complicated to size and calculate. This confronts planners an investors financial and legal uncertainties. Other often reported issues are overheating problems, and related comfort issues, even in winter, (Maiwald 2000) as well as overheating related construction damages (Kerschberger 1997).

Despite these known issues, the author of this paper sees potential in TIM, as nowadays simulation methods make it easier to predict the behaviour of solar facades and to tackle associated difficulties.

 DOI: 10.3217/978-3-85125-786-1-04

MATERIALS AND DATA

3 different TIM have been chosen for the study. These materials are currently market available and represent the most common types of TIM.

Material A

Lumira Aerogel La 1000 by *Cabot*, a transparent silica aerogel granulate which is currently used by many different manufacturers to improve thermal properties of daylight elements (see Figure 2). Detailed transmissivity values were available for layer thicknesses of 15, 25 and 60mm (ZAE Bayern 2010). These have been linearly inter- and extrapolated for other thicknesses. It must be noted that this leads to a growing inaccuracy of data with increasing thickness and tendentially underestimated transmissivity values for high thicknesses.

Material C

TIMax CA by *Wacotech*, a capillary mat, made of modified cellulose acetate (see Figure 3). This material is used in solarthermal collectors and currently not certified for construction purposes. It was still chosen for this study because of the comparatively detailed available data: Direct and diffuse solar transmissivity data was available for all investigated thicknesses (Wacotech, no date). Due to the lack of angular-dependent data, diffuse transmissivity values were used in this study. It must be noted that the light transmissivity of capillary mats is highly dependent on the incident angle with significantly more light being transmitted at low incidence angles. Thus, the use of diffuse transmissivity values does most likely lead to an underestimation of solar gains.

Material G

TIMax GL-S by Wacotech, a light fabric made of a mixture of glass and synthetic fibre (see Figure 4). This material is currently used exclusively in profiled glazing systems. Optical data was only available for two different setups in the form of a g-value (Wacotech 2019 a, b). All values in this study were linearly extrapolated from these two points, the g-value was assumed to be derived from transmission only (g=τs). Due to the poor data basis, results for this material are to be viewed with reservation.

Table 1: Assumed thermal and optical properties of transparent materials, related to layer thickness.

material	d	λ	τ	ρ	α[ii]	g
low-iron glass, outside	0.006	1.00	0.81	0.17	0.02	0.82
low-iron glass, inside	0.004	1.00	0.91	0.08	0.01	0.91
A	0.04[i]	0.02	0.69	0.04	0.27	0.82
Cabot Lumira La1000	0.06	0.02	0.53	0.05	0.42	0.73
Silica aerogel granulate	0.08[i]	0.02	0.37	0.06	0.57	0.65
	0.10[i]	0.02	0.21	0.07	0.72	0.56
	0.12[i]	0.02	0.05	0.07	0.88	0.48
C	0.04	0.08	0.72	0.28	0.00	0.72
Wacotech TIMax CA	0.06	0.10	0.70	0.30	0.00	0.70
capillary mat	0.08	0.10	0.67	0.33	0.00	0.67
	0.10	0.10	0.63	0.37	0.00	0.63
	0.12	0.10	0.59	0.41	0.00	0.59
G	0.04[i]	0.10	0.51	0.49	0.00	0.51
Wacotech TIMax GL	0.06[i]	0.10	0.45	0.55	0.00	0.45
glass & sythetic fibre	0.08[i]	0.10	0.40	0.60	0.00	0.40
	0.10[i]	0.10	0.34	0.66	0.00	0.34
	0.12[i]	0.10	0.28	0.72	0.00	0.28

d…dimension [m] λ…thermal conductivity [W/mK]
τ…transmissivity [-] ρ…reflectivity [-]
α…absorptivity [-] g…g-value (EN 410) [-]
[i] inter- and extrapolated values
[ii] where no detailed data was available, the g-value was assumed to be formed by transmission only (α=0, τ=g)

An overview of thermal and optical properties of all transparent materials defined in the simulations can be seen in Table 1. Note that transmissivity values for outer glass panes have been reduced by the factor of 0.9 and the reflectivity increased accordingly to account for polluted surfaces.

Design variants

For the translucent walls, a mullion-transom steel construction was proposed. The TIM is held between two glass panes (low-iron glass), forming a translucent wall. These wall panels are clamped to a steel sub construction and sealed with EPDM (ethylene propylene diene monomer rubber). To minimize thermal losses, the glass panes are separated by thermally improved spacers (silicone foam). Mullions are assumed to be 60mm wide and spaced 600mm apart, making up for a frame ratio of 10%.

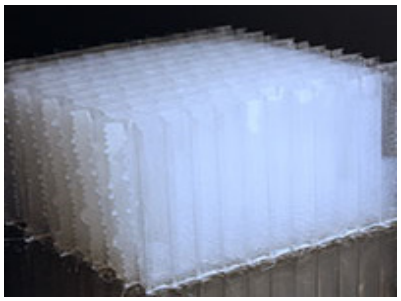

Figure 2: Lumira Aerogel L1000 (system: Solera InsolCore) https://www.advancedglazings.com/products/solera)

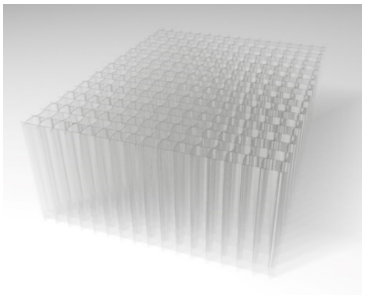

Figure 3: TIMax CA honeycomb by Wacotech (https://www.wacotech.de/sonderanwendung/timax-ca/)

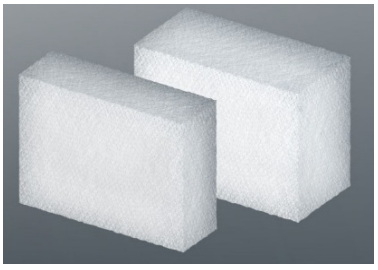

Figure 4: TIMax GL fibre by Wacotech (https://www.wacotech.de/sonderanwendung/timax-gl-glasgespinst/)

 DOI: 10.3217/978-3-85125-786-1-04

For TIM layers up to 60mm the supporting structure was placed behind the translucent wall elements, for higher thicknesses, the steel structure was partly indented into the insulation layer. This was proposed to keep the total construction dimension below 160mm – the diameter of the existing wall system.

Figure shows representative horizontal wall sections of the proposed construction variants. Note that these are design proposals by the author and do not represent recommendations by the suppliers of the TIM.

All proposed wall systems were simulated as translucent walls without thermal mass and as translucent insulation systems in combination with a solar absorbing thermal mass layer (fibre reinforced concrete panels). The proposed thermal mass absorber is separated from the translucent wall by an air gap of 30mm (see Figure 6). This gap can be ventilated to reduce cooling loads and thermal stress on the façade in summer. A maximum solar absorption is achieved by an absorptive coating (α=0.95).

To investigate the influence of thermal mass, 3 different thermal mass layers were simulated in combination with the previously proposed translucent wall systems. Physical properties of the proposed thermal mass layers are listed in Table 2.

In total, 5 different variations of translucent wall systems (TIM-layers of 40, 60, 80, 100 and 120 mm) were combined with 4 variations of thermal mass layers (no thermal mass and thermal mass layers of 20, 40 and 80 mm). These combinations were simulated with the 3 previously described TIM which makes a total of 60 design variants.

SIMULATION APPROACH

The simulations aim to estimate the thermal performance of passive solar walls in the climatic context of Graz and the topographical context of *Terrassenhaussiedlung* under standard conditions of residential use. The simulations focus on heating demands and their possible reduction, overheating and related cooling demands were not addressed at this stage. To avoid situations, where heating and demands alternate and thus the shading strategy becomes a main energy factor, simulations were only carried out for the 4 coldest months of the year (November 1 – February 28).

Thermal bridging

In a first step, the effect of linear thermal bridges between translucent wall panels and their subconstruction was evaluated with the thermal simulation software *HTFlux,* which is validated in accordance with the standards EN ISO 10077-2:2007 and EN ISO 10211-2:2012 (HTflux Engineering GmbH, n.d.). Representative horizontal wall sections of all proposed design variants were built up as shown in Figure 5 with the thermal properties of the 3 proposed TIM to calculate the total thermal resistance R_{total} of the proposed design variants. Punctual thermal bridges (screws) were not considered in the calculation.

Table 2: Properties of thermal mass absorbers

material	Suf.	d	λ	R	ρ	c	c_{eff}
air gap		0.03	0.18	0.17	1.2	1003	-
absorptive coating			α=0.95, ε=0.9				
thermal mass	M2	0.02	2.00	0.01	2200	1000	12.2
fibre reinforced	M4	0.04	2.00	0.02	2200	1000	24.4
concrete	M8	0.08	2.00	0.04	2200	1000	48.9

d…dimension [m] ρ…bulk density [kg/m³]
λ…thermal conductivity [W/mK]
R…thermal resistance [m²K/W]
c…heat capacity [J/kgK] α…absorptivity [-]
c_{eff}…c*ρ*d/3600 [Wh/m²K] ε…emissivity [-]
Suf…Suffix in the naming scheme

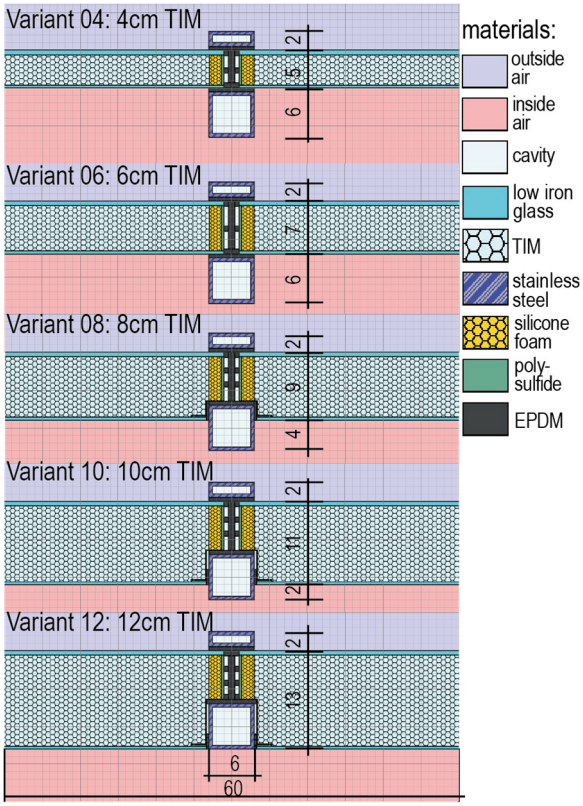

Figure 5: Construction variants of translucent

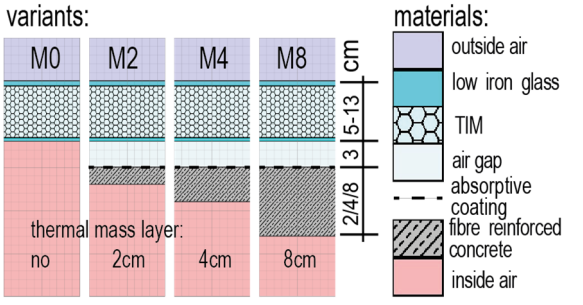

Figure 6: Construction variants of thermal mass

Dynamic simulation

These transferred into a dynamic simulation environment (IESVE). IESVE is validated under ASHRAE standard 140: 2014 and ISO 52000 series of standards (IES, n.d.). Dynamic simulations were carried out in a Level 2 simulation as classified by Eijdems & Poel (1991) and Van Dijk et al. (1991): the

 DOI: 10.3217/978-3-85125-786-1-04

optical properties of the TIM were modelled as a window in front of a mass wall. IESVE's simulation engine calculates optical data at 10-degree intervals and tracks sun rays through transparent elements over multiple reflections and therefore allows a relatively precise modelling of passive solar design strategies (IESVE Help Centre, n.d.).

Representation of constructions

Translucent walls were built up as windows with three panes. While the outer panes represent the actual glass panes, the inner pane represents the thermal and optical properties of the TIM. Thermal resistance of cavities between the glazing layers were set to a minimum. This approach allowed it to transfer the calculated thermal resistances and solar transmissivity values directly into the simulation model. 10% of the wall area were assumed as frame. As the user interface of IESVE the does not allow to specify thermal bridges separately, all thermal bridges were factored into the thermal resistance of the frame R_f (reduction of the resistance to match the overall thermal resistance). Results of these calculations are listed in Table 3.

Geometric representation

All design variants were tested in a simple room model which represents a typical outer zone of an apartment. While variants without absorber walls were modelled as single-zone models, variants with absorber walls were modelled as 2-zone models: A slim unconditioned outer zone, representing the cavity between the translucent wall and the absorber wall, and a conditioned inner zone, representing the actual room (see Figure 7). These two zones are separated by an interior wall with high solar absorptivity (α=0.95). The thermal resistance of the unconditioned air gap between the absorber and the glazing is defined by the heat transfer resistances between the air and its enclosing surfaces. This resistance has been set to 0.09 m²K/W for both enclosing surfaces to represent a thermal resistance of 0.18 m²K/W (30mm air gap with horizontal air flow, as defined in ISO 6946:2017).

To evaluate the heat flux through the façade, the translucent wall systems were set up on one side of the room, while all other surfaces were set as adiabatic (U=0.0 W/m²K). In this representation the translucent façade system covers 100% of the thermally active building envelope.

To account for the topographical context of the site, several instances of the representative room were oriented towards the main orientations of the building complex (South-East and North-West) and placed in a context of simplified shading geometry. These rooms were then offset at different heights to represent 5 different overshading situations 0°, 10°, 20°, 30° and 40° (see Figure 8). As can be seen in Figure 7, local shading geometry (protruding façade elements) was also considered in the model.

Table 3: Thermal properties of translucent walls

Pref.	d_{total}	frame	R_g	R_f	R_{total}	g	g_{eff}
A	TIM: *Lumira La1000* aerogel						
A-40	0.05	0.10	2.01	0.20	1.30	0.63	0.57
A-60	0.07	0.10	3.01	0.32	1.88	0.58	0.52
A-80	0.09	0.10	4.01	0.30	2.18	0.52	0.46
A-100	0.11	0.10	5.01	0.31	2.45	0.46	0.41
A-120	0.13	0.10	6.01	0.32	2.69	0.40	0.36
C	TIM: *TiMax CA* honeycomb						
C-40	0.05	0.10	0.50	0.22	0.45	0.58	0.52
C-60	0.07	0.10	0.61	0.33	0.57	0.57	0.51
C-80	0.09	0.10	0.81	0.30	0.71	0.54	0.49
C-100	0.11	0.10	1.01	0.29	0.85	0.52	0.47
C-120	0.13	0.10	1.21	0.29	0.98	0.49	0.44
G	TIM: *TiMax GL* fibre						
G-40	0.05	0.10	0.41	0.21	0.38	0.43	0.39
G-60	0.07	0.10	0.61	0.33	0.57	0.39	0.35
G-80	0.09	0.10	0.81	0.30	0.71	0.35	0.31
G-100	0.11	0.10	1.01	0.29	0.85	0.30	0.27
G-120	0.13	0.10	1.21	0.29	0.98	0.25	0.23

d_{total}…total wall thickness [m] frame: frame portion [-]
R_{total}…thermal resistance, total section [m²K/W]
R_g…thermal resistance, glazing [m²K/W]
R_f…thermal resistance, frame [m²K/W]
g…g-value (EN 410) [-] g_{eff}…g*0.9 [-]
Pref…Prefix in the naming scheme

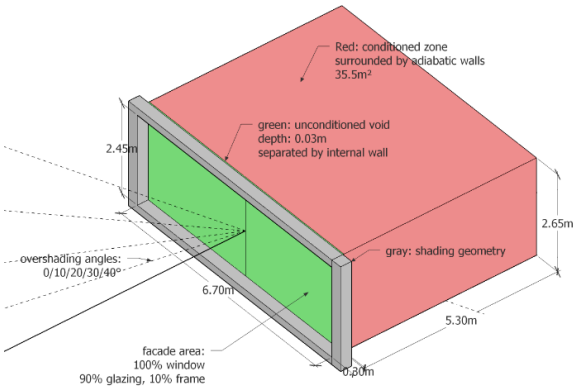

Figure 7: Graphic representation of a representative room, consisting of two zones to represent the double layered façade.

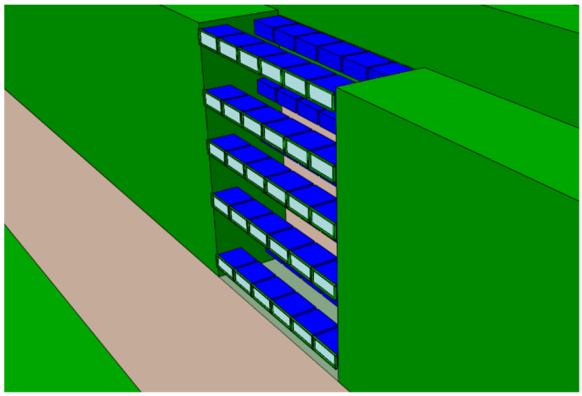

Figure 8: Geometry of the simulation scene, showing a series of identical rooms, representing 5 different overshading situations for the main orientations of the building complex.

 DOI: 10.3217/978-3-85125-786-1-04

Boundary conditions

The following climate data was used for the simulations: Test reference year for the location of Graz, Austria, provided by ZAMG (Zentralanstalt für Meteorologie und Geodynamik). Location: 15°26'52" East, 47°04'47" North, 366m above sea level.
Internal air temperature, Internal loads and air exchanges were set according to the Austrian standard ÖNORM B8110-5: 2019 (see Table 4). As Austrian standards do not provide data for dynamic building simulations, internal loads were modulated according to the Swiss standard SIA 2024:2015, which provides such data. Detailed schedules are shown in Figure 9.

RESULTS

For better understanding of the thermal performance of the proposed design variants, results are represented by two different values: the equivalent conductance of the wall U_{eq} [W/m²K] and the mean heating load of the room Q_m [W/m²].
U_{eq} is derived by dividing the net heat balance of solar gains Q_s and gains/losses through the wall Q_w by the concurrent temperature difference between inside and outside (T_i-T_e) for each simulated hour. Divided by the number of simulated hours n and the façade area A_f one derives a value that describes the average thermal performance of a construction element for a specific period.

$$U_{eq} = \frac{\sum_0^n \frac{Q_s + Q_w}{T_i - T_e}}{n \cdot A_f} \quad (1)$$

For opaque constructions, this value corresponds very well to the calculated U-values as heat flows are mainly driven by thermal conduction. For translucent constructions, this value is highly affected by solar gains and can be negative over certain periods of time, which stands for a heat flow from outside to inside.
U_{eq} does not give a full understanding of the energy performance of a façade, as it does not differentiate between useful gains and gains that merely lead to an interior temperature above the heating set point. Therefore, these results have been contrasted to the mean heating load Q_m which refers to the usable floor area (UFA) of the simulated room.
Figure 10 to Figure 15 show an overview of the simulation results, grouped by TIM. Solid lines stand for variants without thermal mass, dashed lines for results with the highest thermal mass. Not all results are shown in the graphs for better readability. To visualize the effect of solar gains, all design variants were also calculated as opaque elements without solar gains (g-value=0). These results are marked as *g=0*.
For better orientation, all simulation results have been set in relation to simulation results for light-weight opaque walls, which are represented as dashed, blue lines. For example, the line *U0.3* represents the simulation result for an opaque light-weight wall with a U-value of 0.3 W/m²K. *U0.0* stands for the simulation results of a room with no conduction losses, meaning that all heating loads can be attributed to air exchanges. A detailed list of all simulation inputs and outputs is given in Table 5.

Table 4: interior climate conditions for conditioned zones

Heating set point	22	°C
Cooling set point	26	°C
occupancy gains	1.46	W/m² UFA
equipment & lighting gains	2.6	W/m² UFA
ventilation	0.37	ach/h
infiltration	0.11	ach/h
UFA…Usable Floor Area	ach/h… air changes per hour	

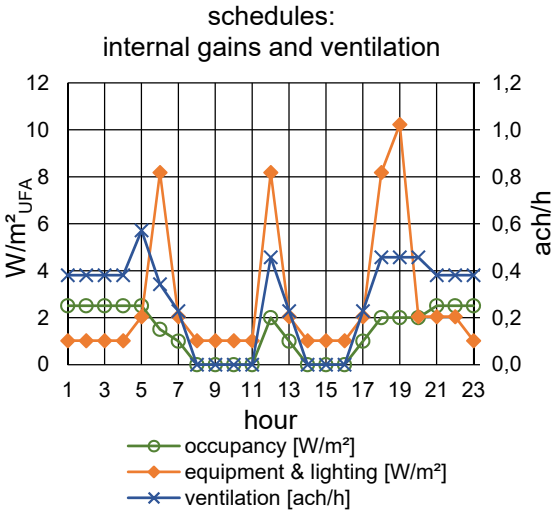

Figure 9: Schedule for occupancy gains used in the simulation

DISCUSSION AND CONCLUSION

The results show that TIM can reach higher thermal standards than any standard insulation materials on well exposed orientations. Even a simple system, as the honeycomb structure *TIMAX CA* can reach positive equivalent U-values and heating loads that are close to a U-value of 0 W/m²K or less (see Figure 13). This is remarkable as this material has been calculated with g-values for diffuse radiation. Since the sun comes at very low angles during the simulated periods and the material shows significantly higher solar transmissivity at such angles, it is very likely, that solar gains have been underestimated.

Influence of U-value and g-value.

For most materials, a lower U-value results in a lower heating load. This effect is most pronounced at orientations with low solar exposure but prevails on all orientations and overshading angles. Seemingly the related decrease of thermal losses outweighs the decrease of solar gains.
A slight exception is the case of the aerogel walls, that show the lowest heating load at 80 mm layer thickness (variants A-08) and an overshading angle of 0° or 10° (see Figure 11). It seems like in these orientations a "sweet spot" between solar gains and thermal losses could be reached. It must be noted though, that the solar transmissivity values for layer thicknesses higher

 DOI: 10.3217/978-3-85125-786-1-04

than 60mm were linearly extrapolated from measured data and could have been underestimated.

Influence of orientation and overshading

As could be expected, the thermal performance of translucent walls is highly deependent on solar exposure. While SE-oriented walls may reach negative equivalent U-values, NW-oriented walls mostly do not reach a thermal performance that can compare to nowadays thermal insulation standards for opaque walls.
The only exceptions are the variants with transparent aerogel (A-04-MX to A-12-MX): even the worst tested orientations perform similar to an undisturbed opaque constuction with the same insulation material. This seems obvious but is still remarkable since the total U-value of the simulated aerogel facades is considerably higher than that of an undisturbed construction due to thermal bridges between frame and glazing (see Table 6).

Influence of thermal mass

More thermal mass in the absorber wall leads to better energy performance. The higher the insolation and the higher the U-value of the translucent wall, the more pronounced this effect is. On orientations that reiceive little solar gains, this effect prevails but can be mostly attributed to the slightly better U-values of the constructions.

Figure 16shows the effect of thermal mass layers on design variants C-04 to C-12 (TIM: TiMax CA) for the best orientation (SE, 00°). To be able to distinguish between the influence of solar gains and the influence of the mass layer alone, the results are contrasted to the same constructions without solar gains (g=0).
While the transparent variants show a decrease of heating load with increasing absober mass, the variants without solar gains only show a significant decrease when a thermal mass layer is added, but no substantial decrease when the thermal mass increases. This initial decrease can be mostly attributed to the additional thermal resistance of the air gap of the air gap between the glazing and the thermal mass.

Outlook

Further simulations are necessary, to test how translucent walls perform in the context of other constructions and construction related thermal bridges. More detailed data, in particular angle-dependent transmissivity values will be needed to receive more founded results. A critical issue that must be adressed is the summer and transition period and related overheating problems. Also practical issues such as costs, noise protection and fire protection must also be taken into account, before final recommenations can be made.

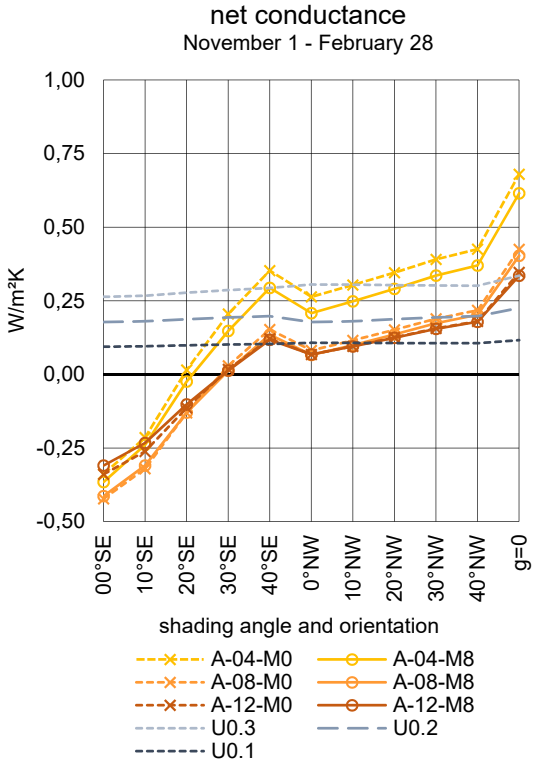

Figure 10: Net conductance in relation to orientation and shading angle for design variants A-04-M0 to A-12-M8

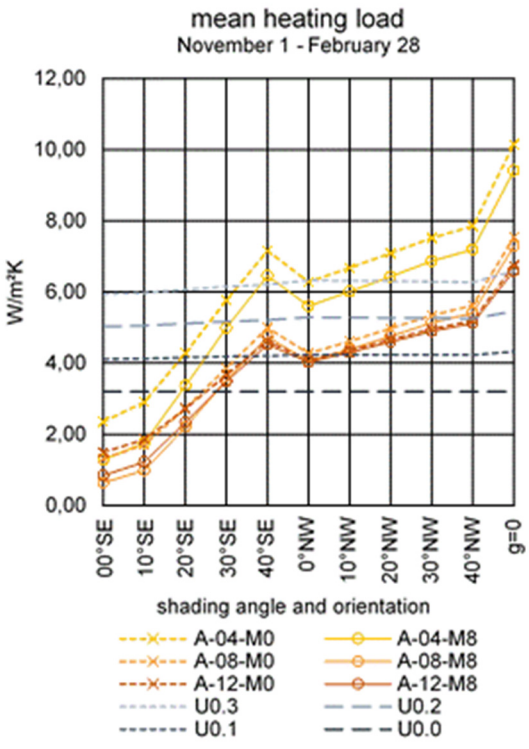

Figure 11: Mean heating load per UFA in relation to orientation and shading angle for design variants A-04-M0 to A-12-M8

 DOI: 10.3217/978-3-85125-786-1-04

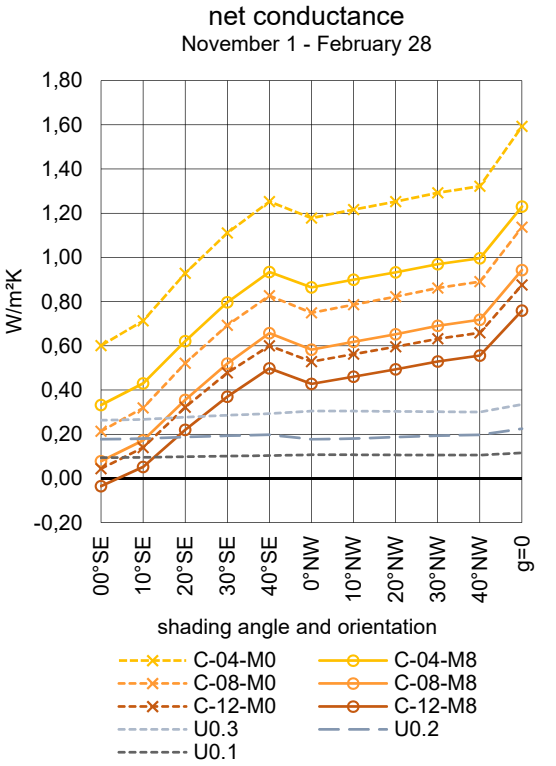

Figure 12: Net conductance in relation to orientation and shading angle for design variants C-04-M0 to C-12-M8

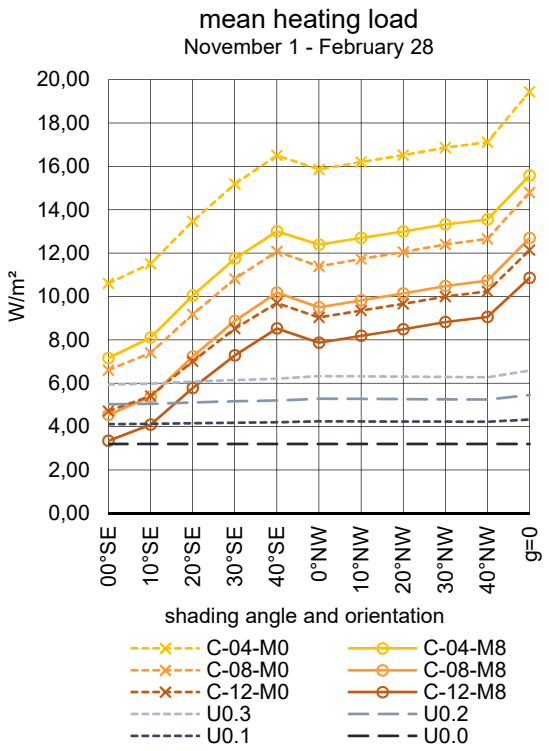

Figure 13: Mean heating load per UFA in relation to orientation and shading angle for design variants C-04-M0 to C-12-M8

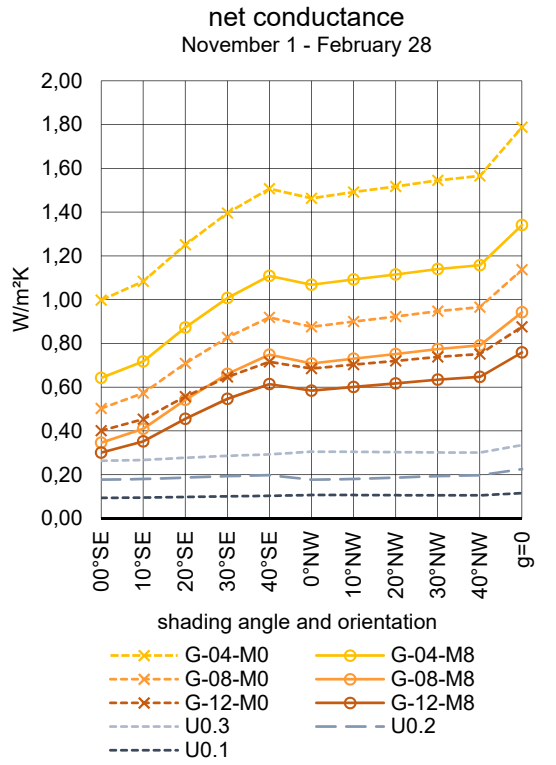

Figure 14: Net conductance in relation to orientation and shading angle for design variants G-04-M0 to G-12-M8

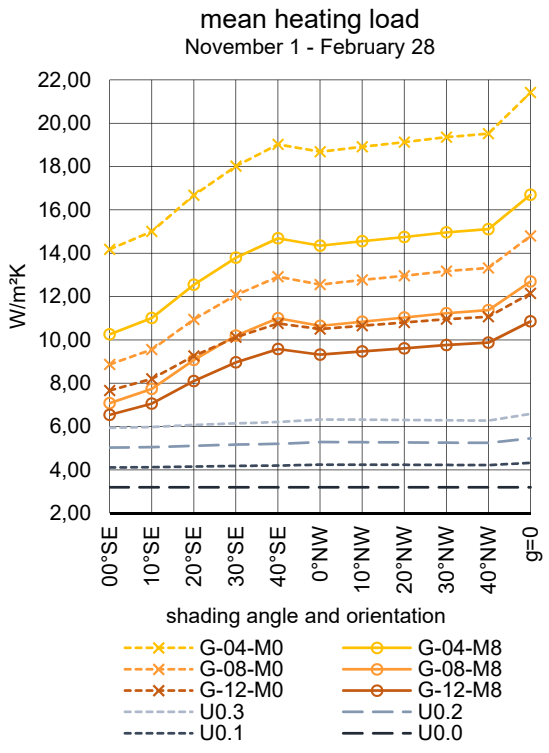

Figure 15: Mean heating load per UFA in relation to orientation and shading angle for design variants G-04-M0 to G-12-M8

 DOI: 10.3217/978-3-85125-786-1-04

Table 5: Simulation inputs and outputs for all design variants (rotate left)

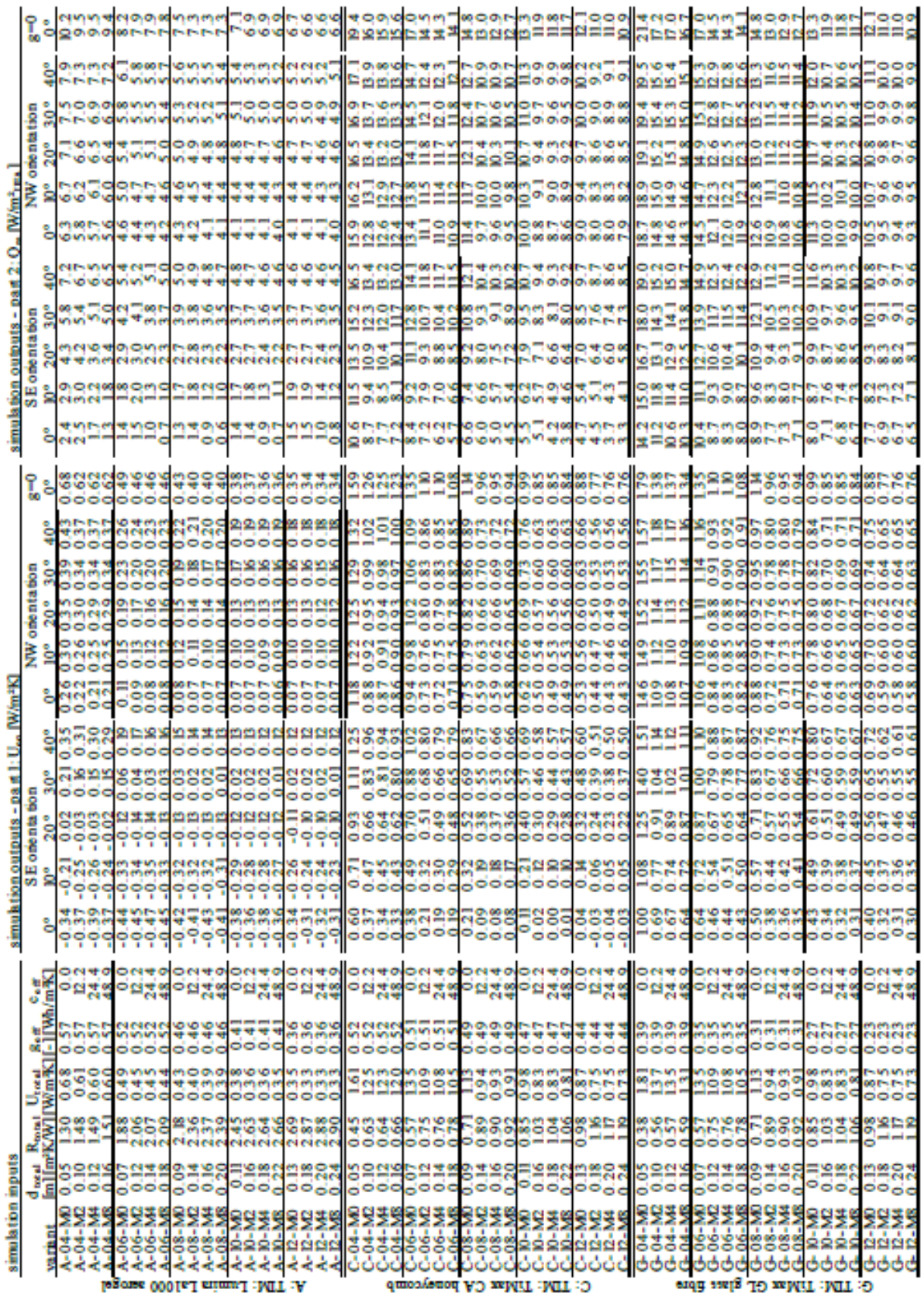

 DOI: 10.3217/978-3-85125-786-1-04

Table 6: Comparison of U-values and mean heating energy demands for transparent aerogel facades and ideal opaque facades with the same insulation properties.

transparent aerogel (NW, 40°)			opaque aerogel		
variant	U_{total}	Q_m	d	U	Q_m
A-04-0	0.68	15.71	40	0.46	15.66
A-06-0	0.49	12.16	60	0.31	12.77
A-08-0	0.43	11.25	80	0.24	11.26
A-10-0	0.38	10.72	100	0.19	10.33
A-12-0	0.35	10.39	120	0.16	9.69

U…overall heat transfer coefficient (U-value) [W/m²K]
U_{total}…U-value, including thermal bridges [W/m²K]
d…dimension [m] Q_m… mean heating load [W/m²UFA]

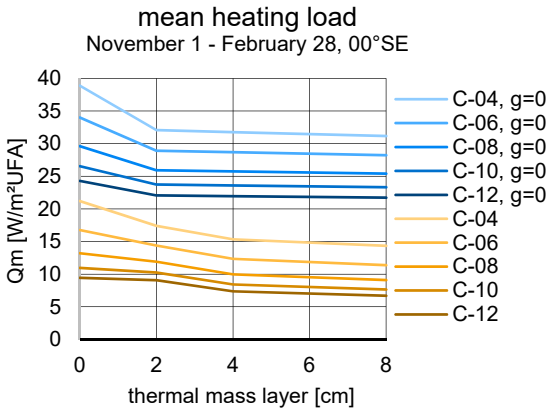

Figure 6: Design variants C-04 to C-12, in comparison to the same wall constructions without solar gains (g=0).

REFERENCES

Čekon M., Čurpek, J., Slávik, R., Šikula, O. 2020. Coupled transparent insulation system with low emissivity solar absorber: An experimentally validated building energy simulation study. Science and Technology for the Built Environment, vol. 26, no. 1, p. 1-13. https://doi.org/10.1080/23744731.2020.1715250

Čekon M.; Čurpek J. 2019. A transparent insulation façade enhanced with a selective absorber: a cooling energy load and validated building energy performance prediction model. Energy and Buildings Vol 183. p. 266-282. https://doi.org/10.1016/j.enbuild.2018.10.032

Eijdems H., Poel A. 1991. Modelling of TIM walls on four levels of detail, Proc. Transparent Insulation Technology Conf. TI4, Birmingham UK.

HTflux Engineering GmbH, n.d. HTflux official webpage, URL: http://www.htflux.com (accessed 07.07.2020).

Integrated Environmental Solutions (IES) n.d. Software Validation, URL: https://www.iesve.com/software/software-validation (accessed 07.07.2020).

Integrated Environmental Solutions (IES) Help Centre n.d. ApacheSim Calculation Methods, URL: https://help.iesve.com/ve2018/apachesim_calculation_methods.htm (accessed 07.07.2020).

Kerschberger, A., Platzer, W., Weidlich, B. 1998. Transparente Wärmedämmung. Produkte, Projekte, Planungshinweise, Bauverlag, Wiesbaden/Berlin Germany.

Maiwald, R. (2000): Die transpaente Wärmedämmung im Spannunungsfel Komfort-Energie und Leistungstest an einer transparenten Wärmeämmung aus einer Isolierverglasung, PhD thesis, Universität Karlsruhe Germany.

Platzer, W. 1998. Advances and Problems of Transparent Insulation in the market. Professionalization and Diversification. EuroSun 98, The Second ISES Europe Solar Congress, Portorož, Slovenia, September 14 - 17, 1998.

Reiss, J., Wenning, M., Ehorn, H. Rouvel, L. 2005. Solare Fassadensysteme. Energetische Effizienz – Kosten – Wirtschaftlichkeit. Fraunhofer IRB Verlag, Stuttart Germany.

Van Dijk, H. A. L., Orersloot, H. O., Bakker L. G. 1991. Thermal-optical modelling of translucent insulation materials – different levels of accuracy, different applications, Proc. Transparent Insulation Technology Conf. TI4, Birmingham UK.

Wacotech (no date). TIMax CA Wabenstruktur, Bauphysikalische Daten, URL: https://www.wacotech.de/sonderanwendung/timax-ca/ (accessed 18.04.2020).

Wacotech 2019a. Datenblatt, System Ug 0.8, URL: https://www.wacotech.de/wp-content/uploads/2019/04/Datenblatt_System08_2019.pdf (accessed 18.04.2020).

Wacotech 2019b. Datenblatt, TWD im zweischaligen Profilglas Standardaufbau, URL: https://www.wacotech.de/wp-content/uploads/2019/04/Datenblatt_zweischalig-Standardaufbau_2019.pdf (accessed 18.04.2020).

Wagner, A. 1998. Transparente Wärmedämung an Gebäuden, Verlag TÜV Rheinland, Cologne, Germany.

ZAE Bayern (Bavarian Center for Applied Energy Research) 2010. Measurment of the transmittance and refelctance of Nanogel samples, commissioned by Cabot GmbH. Report ZAE2-0410-02 (2010), unpublished report.

 DOI: 10.3217/978-3-85125-786-1-04